ELSEVIER

Journal of Nuclear Materials 276 (2000) 90–103

journal of nuclear materials

www.elsevier.nl/locate/jnucmat

Defect accumulation behaviour in hcp metals and alloys

C.H. Woo*

Department of Mechanical Engineering, Hong Kong Polytechnic University, Hung Hom, Kowloon, Hong Kong, People's Republic of China

Abstract

The effects of displacement damage on the physical and mechanical properties of metals and alloys, caused by the bombardment of energetic particles, have been investigated for several decades. Besides the obvious technical and industrial implications, an important motive of such investigations is to understand the factors that differentiate the response of different metals under different irradiation conditions. Recently, much interest is shown in the possible effects of the crystal lattice structure on variations in the damage accumulation behaviour of metals and alloys. In this paper we focus on the case of metals and alloys that crystallize in the hexagonal close pack (hcp) structure, and describe recent understanding of the damage production, accumulation and its consequences in these metals.

1. Introduction

Irradiation damage in crystalline solids due to the impingement of energetic particles occurs in the form of atomic displacements, the initial morphology of which depends on the energy transfer during the impact. For example, MeV electrons produce initial displacement damage in the form of Frenkel pairs, i.e., isolated vacancies and interstitials. Fast neutrons and heavy ions, on the other hand, produce damage in the form of cascades and sub-cascades. The highly localized deposition of the impact energy in the cascade volume in this case produces a large amount of atomic displacements, resulting in a structure that can be described as a high concentration of vacancies and interstitials.

During the collision phase of cascade damage, the course of events is insensitive to the lattice structure, because of the very high kinetic energy of the atoms. However, during the cooling down phase, when the kinetic energy of the atoms is reduced to a level at which a crystal lattice becomes meaningful, further evolution of the cascade structure, and characteristics of its products depend on the lattice structure. This includes the characteristics of the point defects and their clusters, i.e., their number, size, configuration, stability and mobility. As a result, the lattice structure is expected to play a role on the macroscopic behaviour of irradiated materials due to damage accumulation through the kinetics of the reactions among the point defects and their clusters with the existing microstructure.

Historically, the understanding of macroscopic behaviour of materials due to damage accumulation was first established based on reaction kinetics governed by the isotropic migration of vacancies and interstitials. The studies were primarily directed towards cubic metals, in modeling the swelling behaviour due to the growth of irradiation-induced voids. Because of crystallographic anisotropy, isotropic diffusion of the lattice defects in hexagonal close pack (hcp) metals and alloys (simply called hcps in the rest of the paper) can be expected to be the exception rather than the rule. In addition, dislocations with different Burgers vectors are inequivalent in their motion and the reactions with the point defects and their clusters. The geometrical arrangements of sinks relative to the anisotropy of the diffusion then become important factors that dictates the reaction kinetics and damage accumulation behaviour in these materials. This leads one to expect irradiation damage accumulation behaviour very differently from the cubic metals under irradiation.

The purpose of this paper is to review recent advances in the understanding of damage production

* Tel.: +852 2766 6646; fax: +852 2365 4703.
E-mail address: mmchwoo@polyu.edu.hk (C.H. Woo)

0022-3115/00/$ - see front matter
PII: S0022-3115(99)00172-5

and the consequences of its accumulation in the hcps. Wherever possible, the behaviour of cubics will be compared and contrasted.

2. Intrinsic point defects

Similar to the cubic metals and alloys, the elementary intrinsic point defects in the hcp cases are the mono-self-interstitials (simply called interstitials) and the mono-vacancies (simply called vacancies). Much information has been obtained both experimentally, and using computer simulation, concerning the configuration and energetics of these defects in the hcps. The computer simulation results have been reviewed by Bacon [1]. Relevant experimental data have been reviewed and analyzed with reference to the simulation results by Frank [2,3] and Seeger [4]. The reviews are extensive and comprehensive, with the evidence discussed in-depth. For the present purpose, it therefore suffices to simply outline the relevant conclusions reached.

The mono-vacancy takes the simple configuration of a missing atom from a normal lattice site, with a relatively small amount of relaxation in its surrounding. The migration of the vacancy, on the other hand, does not show any evidence of a strong anisotropy in computer simulation studies. From experimental data for six metals, Hood et al. [5] suggested that vacancies might diffuse faster on the basal plane than along the *c*-direction.

The first comprehensive study of energy and stability of interstitials in hcps was performed by Johnson and Beeler [6]. Based on symmetry considerations, the basic interstitial configurations that have been considered are as follows (Fig. 1): the tetrahedral (T), octahedral (O), basal tetrahedral (B_T), basal octahedral (B_O), the basal crowdion (C_B), non-basal crowdion (C_N), the *c*-dumbbell (D_C), the basal dumb-bell (D_B). All computer simulation results indicate the possible existence of multiple stable and metastable configurations, with transition barriers between them well within reach by thermal agitation. The relative stability of the different possible configurations generally depends on the *c/a* ratio. In general, the basal configurations are the preferred stable configurations when *c/a* is less than ideal (i.e., $c/a = \sqrt{8/3}$). On increasing the value of *c/a* from below to above the ideal value, it is expected that the formation energies and stability of the T, O, C_N are the least affected. At the same time, B_T, B_O, C_B and D_B are expected to become less stable with an increase in their formation energy, and D_C to become more stable with a decrease in its formation energy [3]. The migration takes place via in-plane jumps through the configurations B_O, B_T, D_B or B_C, or out-of-plane jumps through the configurations T, O, C_N, D_C. The anisotropy of the interstitial diffusion depends on the diffusivities of the two types of jumps, and is expected to depend on the *c/a* ratio, being weakest for those closest to the ideal ratio.

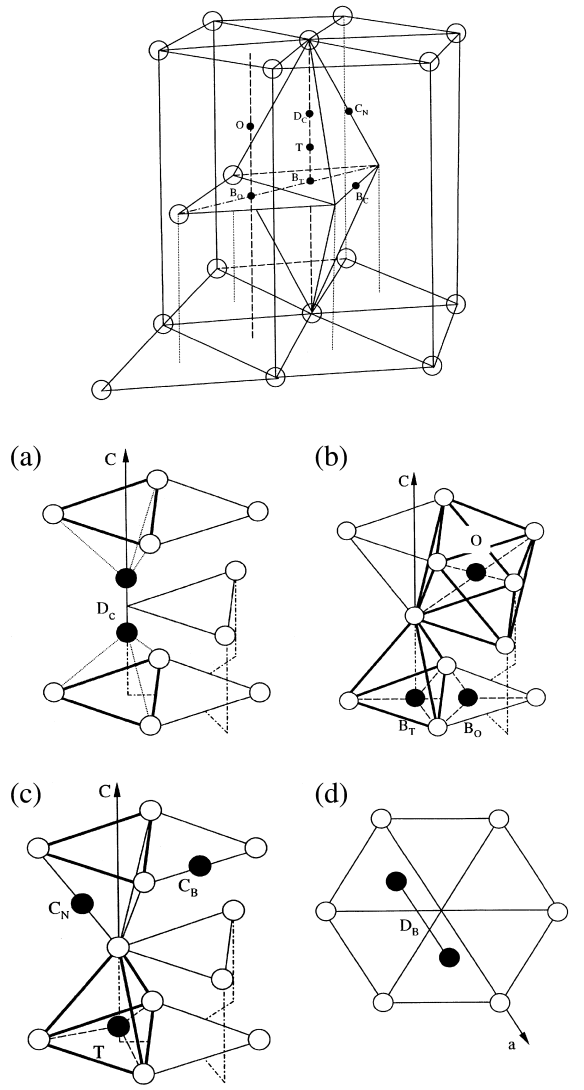

Fig. 1. Possible self-interstitial configurations in the hcp structure.

3. Cascade morphology

As discussed in the introduction, the available evidence suggests that under cascade damage conditions, a substantial portion of the displacements are likely to produce, not single Frenkel pairs, but primary interstitial clusters (PICs) and primary vacancy clusters (PVCs). The intra-cascade clusters play an important role in the kinetics of the reactions that govern the evolution of the

microstructure, and their dual function as both sources and sinks of point defects have to be taken into account. At low temperatures they are predominantly sinks which mainly acts as recombination centers, and at high temperatures they are predominantly sources, particularly the PVCs. The difference between the vacancy clusters and the interstitial clusters in their capacity as point defect sources vary strongly with temperature. Thus, at irradiation temperatures above annealing stage V, vacancies would evaporate from the PVCs and a large fraction of them would enter the medium and contribute to the global vacancy supersaturation. The PICs, on the other hand, are expected to remain thermally stable at least up to temperatures slightly above stage V [7–9], and a significant proportion cannot provide mobile single interstitials to the medium. As a result, the density of the PICs would build up with their continuous production. The observation of damage accumulation suggests that the PICs must have been annihilated at the extended sinks, so that their build-up would saturate at a sufficiently low concentration and they do not become the dominant sink. Woo and Singh [10–12] noticed the large asymmetry that arises in this situation between the *effective* production efficiencies of mobile vacancies and interstitials. They showed that the resulting 'production bias' might provide a large driving force for microstructure evolution. This general philosophy applies, irrespective of crystal structure, to both the cubics and the hcps.

Most results of the MD simulation work on displacement cascades in the hcps are due to Bacon and his group [13–15]. In comparison with the cubics, the general feature of the cascade morphology in the hcps obtained so far is very similar [15]. The number of Frenkel pairs produced as a function of PKA energy is also similar, being much smaller than the total displacements as estimated by NRT [15], and obeying a similar relationship. The cascade morphology is basically the same as the picture derived from the continuum diffusion-reaction calculation reported a decade earlier [16], consisting of single vacancies and interstitials, and their clusters. The vacancy defects are concentrated near the center of the cascade, while those with interstitial characters are near the peripheral. Some clusters are formed at the end of the thermal spike, while others are formed subsequently by short-range diffusion during the next several picoseconds. In the latter case, the diffusion is under the influence of the strong elastic interaction among the interstitials and their small mobile clusters.

Despite the general similarity in the cascade morphologies between the cubics and the hcps, the detailed behaviour of the intra-cascade defects created in the two cases is different because of the different crystal structure. Thus, in the simulations of cascades in both zirconium and titanium at 100 K, interstitials are mostly found in the stable but degenerate D_B and C_B states, and less frequently in the metastable states B_O and C. The migration of the former is preferentially two-dimensional on the basal plane, in contrast to the isotropically migrating dumb-bells in the cubics. Woo [17,18] is the first to point out that the difference in diffusional anisotropy will have significant effects on the evolution of the microstructure and the macroscopic properties of the hcps.

Most small clusters found in the computer simulation of Ti and Zr, both vacancy and interstitial in nature, have the form of perfect prismatic glissile dislocation loops with Burgers vector $\frac{1}{3}\langle 1\,1\,\bar{2}\,0\rangle$. The larger ones have more complex faulted structures, and are sessile. However, this may only be a transient structure on its way to become a perfect prismatic loop eventually, as seen as the most common irradiation damage microstructure seen with TEM. It is interesting to note that defect clusters in the form of basal loops have not been reported in computer simulation studies of cascade initiation in Ti and Zr. This is in contrast to Zn, a metal with $c/a >$ ideal, in which basal loop formation is predicted in the computer simulation of interstitial clustering and observed in TEM work [14].

4. Damage accumulation

The accumulation of irradiation-induced damage in metals and alloys is directly reflected in the evolution of the microstructure, and is observable through the growth of dislocation loops and the voids. Macroscopically, the microstructure evolution produces changes in the dimension and mechanical properties. These effects derived from the damage accumulation can also be observed and measured. In the following available information for these two aspects of damage accumulation in hcps is described.

4.1. Dislocation loops

Although the nucleation and growth of dislocation loops is one of the most prominent features of the accumulation of radiation damage in both the cubics and hcps, there is a significant difference between the two cases. In the cubics, dislocation loops are primarily formed on the close-pack planes ($\{1\,1\,1\}$ for fcc and $\{1\,1\,0\}$ for bcc), and are interstitial in nature. In most cases, the loops are faulted when they are small, but depending on the stacking fault energy and the temperature, the loops may unfault as they grow, by shearing into a configuration of lower energy. In contrast to the cubic cases, both the interstitial/vacancy nature and Burgers-vector structure of irradiation-induced dislocation loops exhibit large variability from one hcp metal to another, due essentially to the differences in the c/a ratio. In particular, the formation

and growth to large sizes of vacancy loops found on some of the hcps is unexpected according to the commonly accepted mechanism of the formation and growth of interstitial loops and voids in the cubics.

Dislocation loops in the hcps nucleates on $\{1\,1\,\bar{2}\,0\}$, $(\{0\,0\,0\,1\})$, $\{1\,0\,\bar{1}\,1\}$ planes in general, with respective Burgers vectors of $\frac{1}{3}\langle 1\,1\,\bar{2}\,0\rangle$, $\frac{1}{6}\langle 2\,0\,\bar{2}\,3\rangle$ (or $\frac{1}{2}[0\,0\,0\,1]$), and $\frac{1}{3}\langle 1\,1\,\bar{2}\,3\rangle$, i.e., a, c and $c+a$. Based on the relative packing densities for different crystallographic planes, the loop habit planes can be correlated with the c/a ratio in the hcp metals [19]. According to whether the principal loop nucleation plane is basal or prismatic, depends on the c/a ratio being greater or smaller than $\sqrt{3}$. This simple rule dictates that except for Zn and Cd, dislocation loops in the hcps should all be prismatic. In reality, the situation under irradiation damage is more complex than that dictated by this simple rule. There are many exceptions. Indeed, basal plane loops have been observed in Mg [20], Zr [21], Ti [22,23], Ru [23], in which the c/a ratio is less than $\sqrt{3}$. In addition, the basal plane loops analyzed in these cases are all vacancy in nature [24]. In Zr and Ti, the situation is further complicated by the co-existence of prismatic loops of both vacancy and interstitial character [25].

Dislocation loops in Zn and Cd have basal habit planes with displacement vectors of $\frac{1}{6}\langle 2\,0\,\bar{2}\,3\rangle$ or $\frac{1}{2}[0\,0\,0\,1]$, and are typically interstitial in character [26]. In Mg, neutron irradiation damage produces both prismatic and basal loops (Fig. 2) [20]. The prismatic loops are interstitial in nature, and the basal loops are vacancy in nature. The irradiation-induced loop structure in Zr and its alloys is probably the most studied among the hcps because of their wide spread use in nuclear reactors. The predominant form of irradiation damage is the $\frac{1}{3}\langle 1\,1\,\bar{2}\,0\rangle$ perfect dislocation loops of both vacancy and interstitial character. The vacancy loops are markedly elliptical whereas the interstitial loops tend to be circular. At 623 K the numbers of interstitial and vacancy loops are almost equal. As the temperature increases, the number of vacancy loops increases, to about 70% at 673 K. A sudden drop of the proportion of a-loops of vacancy character to 20% was observed at temperatures above 723 K. Another characteristic feature of the $\langle a\rangle$-type loops of Zr and Ti caused by neutron, ion or electron irradiation is their alignment in rows or layers parallel with the basal plane (Fig. 3). However, the loop arrangement within the layers is random [27]. There are also reports that the rows or layers are composed predominantly of vacancy loops, with interstitial loops in between the layers [27,28].

Basal plane c-component loops are also commonly observed in the temperature range between 560–773 K. These loops are faulted and are invariably vacancy in nature, having Burger's vector $\frac{1}{6}<2\,0\,\bar{2}\,3\rangle$ (Fig. 4). They are usually large, with diameter between 0.1–1.0 μm. The nucleation and growth of these large vacancy loops is apparently in conflict with the conventional understanding that the point-defect dislocation interaction produces a bias of dislocations for the absorption of interstitials.

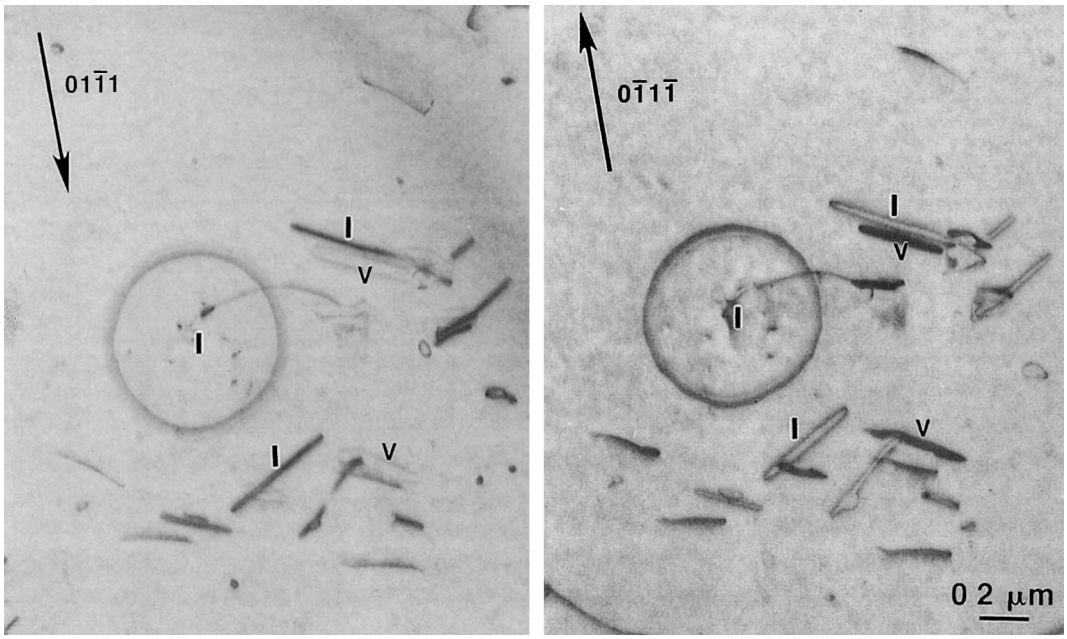

Fig. 2. Dislocation loops in high purity Mg during electron irradiation at room temperature. The loops are prism plane a-loops (interstitial (I) and vacancy (V) in nature). There is also one basal plane c-type loop (interstitial, I) in the center (after Griffiths [59]).

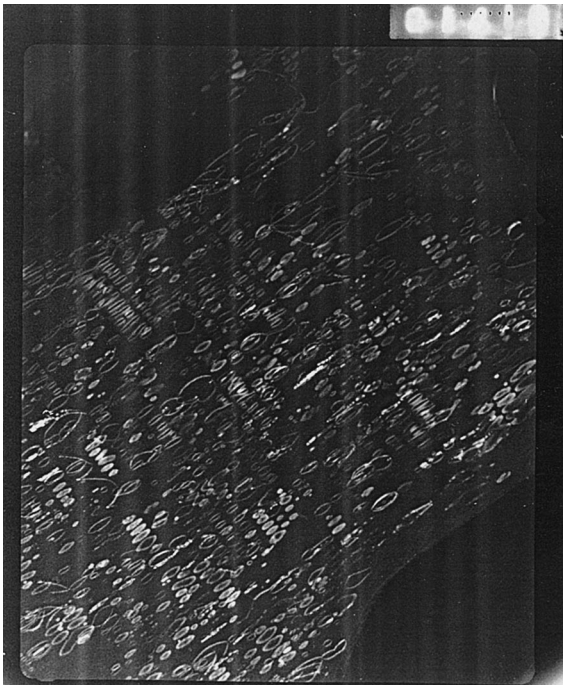

Fig. 3. Loop banding in Ti irradiated at 621 K to a fluence of 4.5×10^{25} nm^{-2}. The Burgers vectors of the loops in any one raft are the same and have the same indices as the plane of the raft (after Griffiths [34]).

Another feature in both neuron (~700 K) and electron (675 K) irradiated Zr is the existence of a zone near grain boundaries which is denuded of interstitial defects. This zone is much bigger than the zone denuded of vacancy defects. Furthermore, the interstitial denuded zone width also depends on the crystallographic orientation of the grain boundary, being wider near basal boundaries than prismatic

4.2. Voids

Void formation has been observed in most hcps, such as electron-irradiated Zn and Co, neutron irradiated Mg [20,30], both neutron and electron irradiated Zr [27,29,31], neutron irradiated Ti [32] and Re [33]. The factors affecting the formation and growth of cavities in the hcps are not very clear. In many cases, the voids are reported to be faceted. For example, the cavities formed in Marz-grade Zr during neutron irradiation in DFR at temperatures between 725 and 740 K were faceted by basal, prism, and pyramidal planes. They are found mostly near grain boundaries inclined to the basal plane [34].

It is interesting to note the morphology change of cavities in Zr at 573 K during their nucleation and growth [35] under electron irradiation in a HVEM. The morphology change, in the form of shortening along the *a*-direction and thickening along the *c*-direction, occurs to cavities generated in Zr samples during a pre-irradiation in DFR at 740 K, and in the electron-irradiated area. In the same experiment, cavities are observed to nucleate adjacent to faulted basal-plane dislocation loops first as thin plates on the basal plane. Subsequent growth of the cavity nuclei occurs by shortening along the *a*-direction and thickening along the *c*-direction (Fig. 5).

4.3. Concomitant deformation

In cubic metals, it is well known that the irradiation-induced climb of dislocations and growth of interstitial loops cause a concomitant volume increase due to the growth of voids. In the presence of an external applied stress, the anisotropy of the dislocation climb and the loop growth causes concomitant deviatoric straining, giving rise to irradiation creep. In addition to void swelling and irradiation creep, in the hcps, the anisotropy of the evolving dislocation structure necessarily produces a deviatoric straining even in the absence of an external stress. Indeed, irradiation growth is the name given to the volume-conserved shape deformation that occurs in non-cubic crystalline materials under irradiation in the absence of an applied stress. The best known examples of irradiation growth are found in graphite [36–39], uranium [40], zirconium and its alloys [41–44]. Irradiation growth in the hcps is a phenomenon corresponding to void swelling in the cubic metals in that it produces dimensional changes in the absence of an applied stress, and that it is caused by the segregation of vacancies and interstitials among two or more kinds of sinks. However, unlike void swelling, each kind of sink produces straining in a different crystallographic direction, such that the final deformation is anisotropic and is volume conserved.

In discussing the deformation of the hcps, it is important to note that the deformation of each grain in a polycrystalline aggregates is constrained by the collective deformation of neighbouring grains, to maintain the integrity of the entire sample. Due to the anisotropy of the deformation of the constituent grains in the hcps, the total macroscopic deformation of a polycrystalline sample cannot be simply taken as an average of the deformation of its individual grains due to the external stress alone [45,46]. Similarly, the irradiation creep and growth components at the single-grain level do not directly translate into the corresponding components at the specimen (polycrystalline) level, which becomes dependent on the texture or crystalline orientation distribution function (CODF). This problem is much less severe in the case of the cubic metals. In the following, unless otherwise specified, experimental samples are polycrystalline.

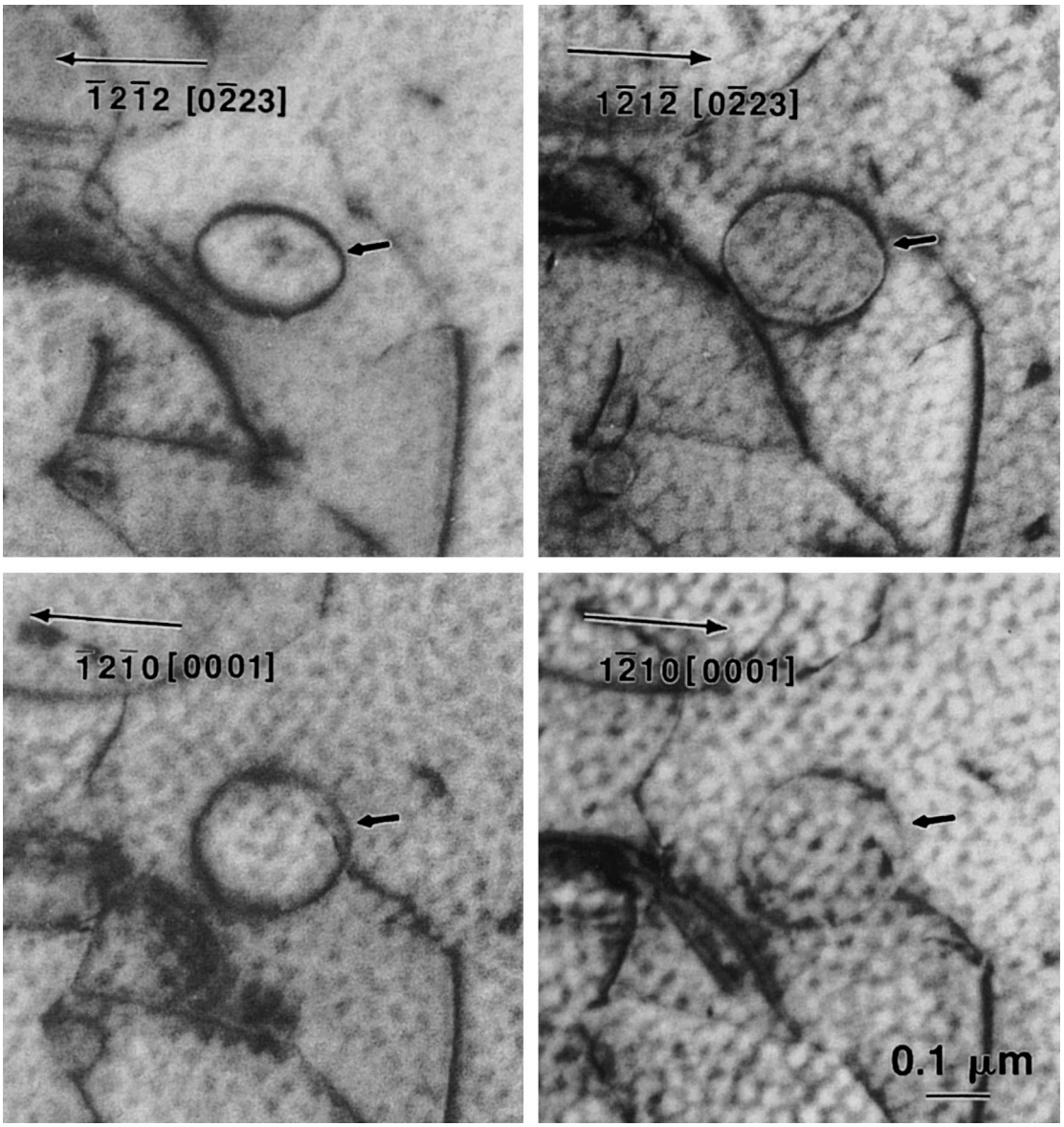

Fig. 4. Basal-plane c-component loop in Zr irradiated in DFR at 740 K to a fluence of 0.2×10^{25} nm^{-2} ($E > 1$ MeV). It exhibits fault contrast with a diffracting vector of $1\ \bar{1}\ 0\ 0$, has a Burgers vector of $\frac{1}{6}\langle 2\ \bar{2}\ 0\ \bar{3}\rangle$ and is vacancy in nature (after [84–86]).

Irradiation creep and growth are investigated in the greatest details in hcp Zr and its alloys, being important - materials for nuclear power reactor components. Irradiation growth in hcp zirconium was first observed in single crystals more than 30 years ago. Since then, experimental data consistently indicated that irradiation growth in polycrystalline zirconium and its single-phase alloys correspond to an expansion along the a-direction and a contraction along the c-direction in its constituent grains [47]. Exceptions, however, are found in alpha–beta alloys such as Zr–2.5Nb and EXCEL [48], in which the grain structure tends to be much finer (sub-micron grain dimensions) and much more anisotropic. It was recently reported that the anisotropy of the growth in these alloys is more complicated, with 'anomalous' cases in which contraction occurs in directions where there is a high concentration of a-axes [49]. Indeed, a 40% cold-drawn and highly stress relieved Zr–2.5Nb alloy showed such anomalous growth anisotropy, with a long-term contraction along both the working and the transverse directions when irradiated at 550 K [49].

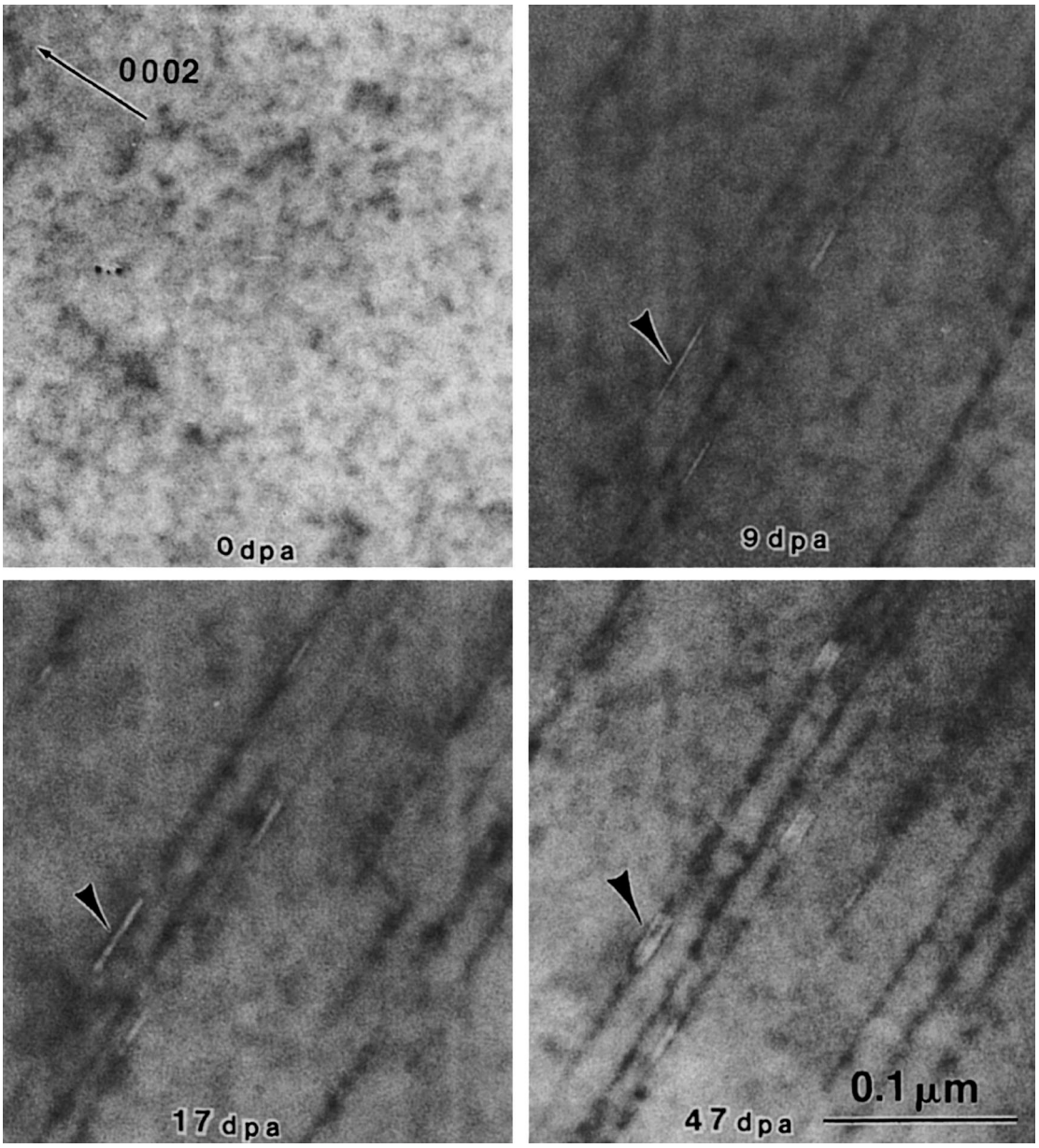

Fig. 5. Electron irradiation of Zr that had previously been irradiated in DFR at 740 K to a fluence of 0.2×10^{25} nm^{-2} ($E > 1$ MeV). Cavities (arrowed) nucleate adjacent to faulted basal plane dislocation loops as thin platelets. Subsequent growth occurs by shortening in dimensions parallel with the basal plane and thickening in dimensions perpendicular to the basal plane.

Irradiation growth measurements for zirconium and its alloys have been performed mainly in the temperature ranges, 50–80°C, 280–400°C and 400–450°C [47,50], which we may refer to as the low, medium and high temperature growth regimes. In addition to the irradiation temperature, the growth rates are also known to be sensitive to the pre-irradiation thermal–mechanical treatment, as well as the microstructure development during irradiation. In general, growth is characterized by an initial transient strain that usually assumes a steady-state at higher neutron fluence, with a constant growth rate.

For annealed 'single-phase' materials like Zircaloy, the microstructure prior to irradiation contains grain boundaries (~10 μm grain size) and a very low network dislocation density (~$10^{13}/m^2$). A high density of *a*-type dislocation loops with normals in the basal plane, of both vacancy and interstitial character, starts to appear

during irradiation. The fraction of a-loops with vacancy character increases with temperature in the low and medium temperature regimes, but drops sharply in the high temperature regime [51]. The growth rate corresponding to this microstructure is relatively low ($<10^{-4}$/dpa in the longitudinal direction). In the medium and high temperature regimes, after some critical neutron dose, which decreases with increasing temperature, faulted c-component vacancy loops appear on the basal plane and the growth rate accelerates [52,53]. In the high temperature regime, the critical dose is so short, and the steady-state growth rates so large, that the distinction between annealed and cold-worked materials narrows [54]. This sharp increase in growth rates in the high temperature regime is remarkably similar to the sharp increase in swelling rates in cubic metals in approaching the peak-swelling regime [55–58].

For cold-worked zirconium alloys, the pre-irradiation microstructure features a and $c + a$ network dislocations as well as grain boundaries [25,59]. Similar to annealed materials an a-loop structure also develops during irradiation. The corresponding growth rates increases with increasing cold work, and are relatively high at all temperature regimes and all fast neutron fluences. For example, the longitudinal growth rate of Zircaloy-4 increases from 3×10^{-4}/dpa in 20% cold-worked material to 10^{-3}/dpa in 78% cold worked material [60]. In some materials, irradiation causes many of the c-component network dislocations to 'split' by climb into partials separated by stacking faults [59]. In other materials, faulted loops form on the basal planes from c-component dislocations undergoing helical climb. The increase in the density of c-component dislocations correlates with an acceleration of the growth rate [61].

Low temperature irradiation-damage annealing studies indicate that at temperatures below 400 K, vacancies in Zircaloy are not mobile [62,63], and diffusion-controlled kinetics predicts only growth in the transient. Indeed, this is experimentally observed in annealed Zircaloy-2 irradiated at 330 K [50]. However, cold-worked Zircaloy-2 shows irradiation growth with significant steady-state rates at these low temperatures [50]. In a related experiment, irradiation growth strain at 350 K of cold-worked Zr specimens containing 3 and 70 ppma iron was measured as a function of proton dose in a 4.4 MeV proton beam at the Whiteshell Laboratory [64]. There is no difference in the irradiation deformation rate between the two types of specimens. In both cases, the deformation rate was found to be linearly dependent on the dose rate.

Application of a sufficiently high stress in general causes thermal creep to become significant in metals. Irradiation damage produces two effects. On the one hand, irradiation hardening retards thermal creep in annealed materials stressed near or above the yield stress. At the low temperature regime, on the other hand, irradiation-induced mechanisms significantly lower the stress level at which creep becomes important. In the case of hcps such as Zr, both the irradiation-induced or thermal creep is anisotropic, reflecting the crystallographic anisotropy [47]. Compared to the cubic metals, the major difference of creep in the hcps is the anisotropy. Indeed, for constant stress, temperature and flux, the irradiation creep rates of zirconium alloys are usually higher in the direction of working [65]. Using a self-consistent model to take into account the intergranular interaction, the analysis of irradiation-induced deformation data of zirconium alloys [45,46,66] shows that at the grain level the irradiation creep compliance is largest for a prismatic shear load. The creep compliances due to the tetrahedral and basal shear modes are usually much smaller, and in many cases, the creep compliances for different stress modes can differ by an order of magnitude. In general, the creep compliances for all stress modes increase with the amount of cold work. However, the tetrahedral shear mode seems to be more affected by pre-irradiation rolling than by tensile deformation [66]. This is best illustrated [66] by measurements performed on three types of samples: (a) annealed Zircaloy plate; (b) specimens from (a) that were cold-worked 1.5% in tension; and (c) specimens from (a) that were cold-worked 1.5% by rolling. These samples were irradiated at the ATR reactor at Idaho falls at a fast flux of about 2×10^{18} nm^{-2} s^{-1} at a temperature of $\sim$330 K. The transient irradiation growth behaviour was analyzed by taking into account the role of the inter-granular interaction using the self-consistent model [66]. The resulting creep compliances were reproduced in Table 1, with the densities of the a- and c-types dislocations, for comparison.

The data in Table 1 is consistent with the straightforward interpretation that the creep compliance under the tetrahedral shear (i.e., $k^{(1)}$) is mostly related to the c-type dislocations, while that under the prismatic and basal shears (i.e., $k^{(2)}$ and $k^{(3)}$) are more related to the a-type dislocations. We note that dislocations that belong to the pyramidal system, i.e., $c + a$ dislocations, are included in both the c- and a-types.

Table 1
Dislocation Densities (in units of 10^{14} m^{-2}) and creep compliances (in units of 10^{-9} Mpa^{-1} h^{-1}) of three types of samples made by different prior mechanical treatment of the same material, showing the dependence of the creep complaince on dislocation structure

	Annealed	1.5% tensile	1.5% rolled
$\rho(a)$	0.23 (92%)	0.87 (87%)	0.74 (74%)
$\rho(c)$	0.02 (8%)	0.13 (13%)	0.26 (26%)
$k^{(1)}$	0.2	1.0	3.0
$k^{(2)}$	12.0	24.0	24.0
$k^{(3)}$	8.0	16.0	16.0

5. Point-defect kinetics

A main assumption implicitly made in the usual rate theory for cubic metals is that the diffusion of point defects is isotropic. Since the migration of point defects in the hcps are likely to be anisotropic because of the crystal structure, the usual rate theory is not expected to be adequate in describing the irradiation damage behaviour of the hcps, because of the incorrect reaction kinetics. To address this problem, Woo and Goesele [67] generalized the rate theory for application to hcps metals like Zr, using the reaction kinetic theory of anisotropically diffusing reactants. It was found that the difference in diffusional anisotropy (DAD) [17,68] between vacancies and interstitials can produce a large bias in their reaction rates with sinks. This bias is a zero-order effect and may completely dominate the conventional dislocation bias caused by the first-order elastic interaction between the point defects and the sink. In contrast to the usual rate theory model based on the assumption of isotropic point-defect diffusion, the bias for edge dislocations in the hcps depends on their line directions, and need not be biased towards interstitials. Further investigations found that [17,18] grain boundaries and surfaces are also strongly biased towards the vacancies or interstitials according to their crystallographic orientations. This large variability of biases for sinks adds another dimension to the complexity of irradiation damage behaviour to the hcps. It has been shown [17,35,67–69] that the DAD leads to many of the anomalous behaviour of growth in zirconium. As an essential tool for the understanding irradiation damage in the hcps, the methodology for treating reaction kinetics in an anisotropic diffusive medium during irradiation is briefly reviewed in the following (for more details the interested reader is referred to [17]).

Reactions among mobile defects and between mobile defects and sinks in a solid may be modelled by a kinetic theory similar to the one that governs the chemical reactions between molecules diffusing in a solvent. Based on the classic works of Smoluchowsky [70], Onsager [71] and Debye [72], Waite [73] developed an elegant formulation of the reaction kinetics of diffusion-influenced reactions within the concept of a pair probability function. Using this formulation, Goesele and Seeger [74] developed a theory for the bimolecular reaction rates in an anisotropic diffusion medium. It was shown that the anisotropic diffusion problem can be reduced to a simpler isotropic diffusion problem in a modified co-ordinate system, with a transformed reaction volume that has a different shape (but the same magnitude) as the original reaction volume.

The reaction among irradiation generated defects and their annihilation at sinks can be represented by the bimolecular reaction between two reacting species A and B of the form

$$\mathrm{A} + \mathrm{B} \rightarrow \mathrm{C}, \tag{1}$$

where at least one of the species is diffusible and the reaction product C is assumed to have no influence on the further reaction process.

Starting with randomly distributed reactants having anisotropic diffusion tensors $\mathbf{D}^{\mathrm{A}}$ and $\mathbf{D}^{\mathrm{B}}$, and an interaction potential $U(\mathbf{r})$ between A and B, the progression of reaction (1) (i.e., the chemical kinetics) is completely governed by the following law of mass action

$$\dot{C}_{\mathrm{A}} = \dot{C}_{\mathrm{B}} = -\bar{D}\alpha(t) C_{\mathrm{A}} C_{\mathrm{B}}, \tag{2}$$

where the dots over C_{A} and C_{B} denote the time derivative, and

$$\bar{D} = (D_x D_y D_z)^{1/3} \tag{3}$$

with D_x, D_y and D_z, being the principal values [75] of the relative diffusion tensor $\mathbf{D}$, which is assumed to be constant m space and time, and where

$$\mathbf{D} = \mathbf{D}^{\mathrm{A}} + \mathbf{D}^{\mathrm{B}}. \tag{4}$$

Eq. (2) holds independent of the boundary conditions on the reaction volume. The reaction coefficient $\alpha(t)$ is a function of time given by

$$\alpha(t) = \frac{1}{\Omega} \int (\nabla\phi + \beta\nabla U)\, \mathrm{d}S, \tag{5}$$

where Ω is the atomic volume. The integral extends over the surface S of the transformed reaction volume. For three-dimensional diffusion, the transformation reads

$$x = \sqrt{\frac{\bar{D}}{D_x}} x_0, \quad y = \sqrt{\frac{\bar{D}}{D_y}} y_0, \quad z = \sqrt{\frac{\bar{D}}{D_z}} z_0, \tag{6}$$

where x, y, z are the transformed, and x_0, y_0, z_0 the original, Cartesian co-ordinate system parallel to the principal axes of $\mathbf{D}$. The case for lower-dimensional diffusion (i.e., when one or more of the D_x, D_y, D_z vanishes) is similar. β is the reciprocal of the product of the Boltzmann's constant and the absolute temperature. The quantity ϕ in Eq. (5) is related to the pair probability density ρ_{ij} between reaction partners i and j [74]. Expressions for $\alpha(t)$ for many interesting cases have been derived in the literature [76]. If B is an indestructible sink such that $\dot{C}_{\mathrm{B}} = 0$ then Eq. (2) applies only to $\dot{C}_{\mathrm{A}}$.

During irradiation, point defects are continuously being generated and subsequently annihilated, and the concept of pair probability densities discussed above is not applicable. However, under steady-state conditions, it is possible to derive a time-independent effective reaction coefficient α from the time-dependent annealing reaction coefficient $\alpha(t)$. Using the concept of an effective lifetime, under continuous generation conditions, the steady-state reaction coefficient α can be defined by [77]

$$\alpha = \tau_{\text{eff}}^{-1} \int_0^\infty \alpha(t)\, \exp(-t/\tau_{\text{eff}})\, \mathrm{d}t, \tag{7}$$

where τ_{eff} is the mean time until annihilation of a point defect of the species, whether through spontaneous or induced conversion, recombination with the anti-defect, or disappearance in a sink. Within the effective medium approximation, τ_{eff} is the lifetime of a point defect before its absorption in the lossy medium [77].

Replacing $\alpha(t)$ by α, Eq. (2) becomes the steady-state kinetic equation under continuous generation conditions. For the single-sink situation the reaction constants calculated by Eq. (7) are equivalent to those calculated by an effective-medium approach [77]. If B is an indestructible sink in Eq. (1), then αC_{B} is equal to the usual sink strength k_{B}^2 within the effective medium approximation [77]. Woo [17] showed that a difference of α for the sink B between the vacancy and the interstitial will produce a bias of the sink B, and a driving force for microstructure evolution.

The lifetime of individual process is also related to the corresponding reaction coefficients according to

$$k_{\text{B}}^2 = \alpha C_{\text{B}} = (\bar{D}\tau_{\text{B}})^{-1}. \tag{8}$$

The relationship between the total sink strength, the mean effective lifetime and the lifetime of the individual processes are then given by

$$k^2 = \sum_{\text{B}} k_{\text{B}}^2 = (\bar{D}\tau_{\text{eff}})^{-1}, \tag{9}$$

where

$$\tau_{\text{eff}}^{-1} = \sum_{\text{B}} \tau_{\text{B}}^{-1}. \tag{10}$$

5.1. Diffusional anisotropy difference (DAD)

Goesele [76] assembled a list of factors affecting the value of α:

- size and shape of reaction volume;
- boundary condition imposed on the reaction volume, i.e., whether reaction takes place immediately on contact, or is delayed because of an energy barrier;
- attractive or repulsive interaction between reaction partners;
- anisotropy and dimensionality of diffusion;
- continuous generation of reaction partners;
- parallel reactions, i.e., reaction to the A–B reaction, reaction with other partners;
- spontaneous decay, i.e., point defect having a finite lifetime because of conversion from an excited state, or annihilation;
- geometric arrangement of a reaction partner species, i.e., random distribution or in a regular array;
- spatial correlation, e.g., correlated recombination between Frenkel pairs.

In cases where the point-defect diffusion is isotropic, the most obvious difference between the reaction constants of vacancies and interstitials originates (see Eq. (5)) from the difference in U – the point-defect/sink interaction between the vacancies and the interstitials. Thus, edge dislocations have a bias for interstitials because the corresponding U is usually larger for the interstitials than for the vacancies because of the larger size-effect interaction. Voids are neutral sinks because the corresponding U is negligible for both kinds of point defects. In an irradiated material with voids and edge dislocations the voids will grow because of a net flux of vacancies. At the same time, interstitial loops will grow and edge dislocations will climb because of a net flux of interstitials. This is the conventional picture generally believed to be the mechanism responsible for void swelling.

The situation is very different in the hcps. Due to the crystallographic anisotropy of the hcps, both the jump distances and the successful jump rates depend on the jump directions. In this case, the reaction constants depend on the diffusional anisotropy through the transformed reaction volume in Eq. (5) and the bias must also depend on the difference in the diffusional anisotropy between the vacancies and the interstitials. More importantly, the biases that originate from the Diffusional anisotropy difference (DAD) are zero-order effects, and are expected to play a dominating role in the irradiation-induced microstructure evolution and macroscopic deformation in the hcps. Our experience with cubic metals, such as that edge dislocations are biased towards interstitials, grain boundaries and surfaces are neutral sinks, etc., must be generalised before it is applicable to the hcps.

The effect of DAD may be illustrated by the following example. Let us consider a random distribution of spherical voids of radius R in a medium in which diffusion obeys cylindrical symmetry. Let D_c and D_a be the diffusion coefficients in the longitudinal and transverse directions, respectively. Suppose the diffusivity of the vacancy is moderately anisotropic, i.e., $0.1 < D_a/D_c < 10$, and that of the interstitials is preferably one-dimensional, i.e., $D_a/D_c \ll 1$, and the elastic interaction between the point defect and the sinks is negligible. For cases where the sink separation is much larger than the void radius, we have

$$\alpha_v = \frac{4\pi}{\Omega} R, \quad \alpha_i = \frac{8}{\Omega}\left(\frac{D_c}{D_a}\right)^{1/6} R. \tag{11}$$

The bias of the void can be calculated [17]. For a value of $D_a/D_c = 0.01$, for example, the void has a 27% bias towards interstitial. This bias is entirely due to DAD, and is very substantially different from that derived from the traditional rate theory, in which the voids are neutral sinks. It is clear that DAD would produce a substantial

difference between the irradiation damage in cubic and hcps metals.

Expressions for typical sink geometry have been derived previously [17]. Nevertheless, for convenience of discussion, we summarise the main results in the following:

Let D_c and D_a be the principal diffusivity along and orthogonal to the c- and a-axes, respectively. For spherical sinks with radius R, the reaction constant is given by the following equations:

$$\alpha = \frac{8}{\Omega}\left(\frac{D_c}{D_a}\right)^{1/6} R\left[1 + \frac{\pi R}{4\sqrt{\bar{D}_a \tau_{\text{eff}}}}\right] \quad \text{for } D_c \gg D_a, \tag{12a}$$

$$\alpha = \frac{4\pi}{\Omega} R\left[1 + \frac{R}{\sqrt{\bar{D}\tau_{\text{eff}}}}\right] \quad \text{for } D_c \approx D_a, \tag{12b}$$

$$\alpha = \frac{4\pi}{\Omega}\left(\frac{D_a}{D_c}\right)^{1/3} R\left[\left(\ln\sqrt{4\frac{D_a}{D_c}}\right)^{-1} + \frac{\pi R}{4\sqrt{D_a \tau_{\text{eff}}}}\right] \quad \text{for } D_c \ll D_a, \tag{12c}$$

$$\alpha = \frac{2\pi R^2}{\Omega\sqrt{D_c \tau_{\text{eff}}}} \quad \text{for} \quad D_a = 0, \tag{12d}$$

$$\alpha = \frac{8\pi R}{\Omega \ln\left(4D_a\tau_{\text{eff}}/\pi R^2\right)} \quad \text{for } D_c = 0. \tag{12e}$$

For cylindrical sink such as line dislocations, the orientation of the sink is defined by the angle λ between the cylindrical axis of the sink and the symmetry axis, i.e. c-axis, of the diffusion field. It is convenient to measure the diffusion anisotropy by a parameter p given by

$$p = (D_c/D_a)^{1/6}. \tag{13}$$

Then the reaction constant per unit length for a cylindrical sink α_d is given by [68]

$$\alpha_d = \alpha_0 p^{-2}\left(\cos^2\lambda + p^6 \sin^2\lambda\right)^{1/2}, \tag{14}$$

where α_0 is the corresponding reaction constant for isotropic diffusion

$$\alpha_0 = \frac{2\pi}{\Omega \ln\left[\sqrt{4\pi^{-1}\bar{D}\tau}/R\right]}. \tag{15}$$

It is clear from Eqs. (12a)–(12e) that the difference in p between the vacancies and the interstitials produces a strong bias on top of the usual dislocation bias contained in α_0. Furthermore, this bias is a function of the orientation of the dislocation with respect to the diffusion field.

Let us now consider the case of planar sinks, which are often used to simulate grain boundaries and surfaces. We consider a pair of parallel planes separated by a distance $2d$ by a diffusive medium in which the point defect lifetime before annihilation is τ_I. Let $\hat{\mathbf{n}}$ be the unit normal vector to the plane. Suppose in the principal system of the diffusion tensor,

$$\hat{\mathbf{n}} = \begin{pmatrix} \sin\lambda\cos\phi \\ \sin\lambda\sin\phi \\ \cos\lambda \end{pmatrix}, \tag{16}$$

where λ and ϕ are respectively the polar angle and the azimuthal angle of $\hat{\mathbf{n}}$ in the principal system of the diffusion tensor. The sink strength of the pair of surfaces is given by

$$k_s^2 = \frac{k_I}{d'}\left[\coth(k_I d') - \frac{1}{k_I d'}\right]^{-1}, \tag{17}$$

where k_I^2 is the effective medium sink strength of the medium and is related to τ_I according to Eq. (10), and d' is defined by

$$d' = \sqrt{\frac{\bar{D}}{D_n}}d \tag{18}$$

with D_n given by

$$D_n = \begin{cases} \bar{D}p^{-2}(\sin^2\lambda + p^6\cos^2\lambda) & 3D: D_c \neq 0;\ D_a \neq 0 \\ \bar{D}\sin^2\lambda & 2D: D_c = 0;\ D_a \neq 0 \\ \bar{D}\cos^2\lambda & 1D: D_c \neq 0;\ D_a = 0 \end{cases} \tag{19}$$

These results can be applied to calculate the sink strength of grain boundaries. Let $2d_x$, $2d_y$ and $2d_z$ be the dimension of the grain in the shape of a parallelepiped along the principal directions of the diffusion field corresponding to the diffusion coefficients D_x, D_y and D_z. The sink strength k_α^2 of the pair of boundaries S_α with surface normals along the α^{th} direction is given by the set of transcendental equations in k_x^2, k_y^2 and k_z^2:

$$k_\alpha^2 = \frac{\sqrt{(k^2 - k_\alpha^2)}}{d'_a} \times\left\{\coth\left[d'_\alpha\sqrt{(k^2 - k_\alpha^2)}\right] - \frac{1}{d'_\alpha\sqrt{(k^2 - k_\alpha^2)}}\right\}^{-1}, \tag{20}$$

where

$$d'_\alpha = \left(\bar{D}/D_a\right)^{1/2} d_\alpha \quad \text{and} \quad k^2 = k_x^2 + k_y^2 + k_z^2 + k_I^2. \tag{21}$$

6. Discussions

It is clear from the foregoing discussions that the difference in diffusional anisotropy between the vacancies and the interstitials, as expressed by p, produces a

difference in the corresponding sink strength, resulting in a sink bias. More importantly, this bias is a function of the orientation of the sink with respect to the diffusion field. Thus, edge dislocations and loops in hcps do not necessarily have a bias towards interstitials as in the cubic metals. Its bias depends on the orientation of its line directions with respect to the crystallographic direction, and may be towards the vacancies. Even voids in general are not neutral sinks, but have biases depending on the void shape and diffusion anisotropy. Similarly, surfaces and grain boundaries also have biases that depend on their orientations. Furthermore, even different parts of the surface of a void, or of the line of a dislocation loop, may have different biases corresponding to the different orientations with respect to the diffusion field, so that loops and voids may maintain a thermodynamically unfavourable shape under irradiation. Based on this simple picture, most features of irradiation damage in the hcps as described in Section 4 can be understood. Thus, the growth of vacancy loops to large size (despite the conventional bias towards interstitials due to the elastic interaction), the large variability in the correlation of loop nature (i.e., vacancy or interstitial) with the Burgers vector, and the observation that voids in Zr nucleate as thin discs on the basal planes which subsequently thicken and decrease in width, are natural consequences of DAD.

As mentioned earlier, TEM examination of neutron-irradiated zirconium [28,33,78] and titanium [79,80] samples reveal that, the loops are elliptic. However, the ellipticity is different between the vacancy and the interstitial loops, i.e., the vacancy loops are elongated along the *c*-axis, whereas the interstitial loops are almost circular. Post-irradiation annealing [80] reduces the ellipticity difference between the two types of loops.

In an elastically isotropic medium, minimum line tension dictates that a dislocation loop is circular in thermal equilibrium. When the medium is elastically anisotropic, the equilibrium shape of a dislocation loop is generally elliptical, the ellipticity depending on the anisotropy and is the same for both the vacancy loops and interstitial loops [33].

Under irradiation conditions, the shape of a dislocation loop also depends on the kinetics of point defects reacting with the dislocation loops. This is particularly true in the presence of a high jog density in the loop, so that point defects can be considered annihilated at the point where it enters the dislocation loop. We have seen that the bias of a dislocation line is in general a function of the line direction. This may give rise to a bias differential among different segments of the same dislocation loop, so that different segments may receive a different net flow of interstitials. It is not difficult to see that this also causes loop ellipticity.

Loop ellipticity caused by DAD can be distinguished from that caused by elastic anisotropy. First of all, loop ellipticity due to DAD would be different between vacancy and interstitial loops. In fact, in the absence of elastic anisotropy, the major axis of the elliptical loops of vacancy and interstitial characters would be orthogonal to each other. Secondly, post-irradiation annealing should remove the difference between the ellipticity of vacancy and interstitial loops. This observation can be understood if we assume that elastic anisotropy causes the loops (both vacancy and interstitial) to be elongated along the *c*-direction. Then, for an interstitial that migrates faster on the basal plane than along the *c*-direction, vacancy loops grow faster in the *c*-direction than the *a*-direction (increasing their ellipticity). The situation is reversed for the interstitial loops. It can be seen that the superposition of the dynamic DAD effect and the static elastic effect would produce the required difference m ellipticity, as observed.

Another interesting phenomenon is the spatial ordering of loops in hcps. Spatial correlation of microstructure is often observed in irradiated crystalline solids. The most spectacular example is perhaps void-lattice formation. It has been suggested [81–83] that void lattices form as dissipative structures in open systems due to kinetics, and not due to the attainment of thermodynamic equilibrium. DAD is the mechanism that is instrumental in bringing about this kind of ordering. Thus, the operation of DAD in hcps may also exhibit itself in the spatial correlation of microstructures. We have seen in earlier sections that dislocation loops in Zr and Ti also exhibit such ordering phenomena.

Such ordering phenomena can be understood in terms of DAD. Every point defect spends a finite time migrating in the lattice between its generation by irradiation and its subsequent annihilation by mutual recombination or at a sink. During its lifetime it can only travel a finite distance s from its point of creation. Thus, all the point defects that are subsequently annihilated at a sink have to be created within a distance *s* from the sink, i.e., in a volume centred on the sink. We call this volume the point-defect capture volume of the sink. For a spherical sink, for example, its capture volume is spherical for the isotropic point-defect mobility and is ellipsoidal if otherwise. The vacancy and interstitial capture volumes would be different if there is a DAD between the vacancies and the interstitials. The overlapping of capture volumes between neighbouring sinks reduces the corresponding point-defect flux to the sink. Thus, vacancy sinks, for example, will grow faster if neighbouring sinks are situated in such a way that the interstitial flux to the sink is reduced without significantly affecting the vacancy flux. The resulting growth rate differential would cause a Darwinian selection, giving rise to a spatial correlation between the sinks.

Thus, vacancy loops that are closer on the basal plane than on the *c*-axis would share their interstitial capture volumes on the basal plane while avoiding

overlap of their vacancy capture volumes along the *c*-direction. These vacancy loops would grow faster. Similarly, interstitial loops would grow faster if they avoid each other on the basal plane and get closer in the *c*-direction. This may be a contributing reason for the observation of aggregation of vacancy loops into bands on the basal plane, and interstitial loops into prismatic rafts in neutron-irradiated zirconium described earlier in this paper. This also allows the simultaneous growth of vacancy and interstitial prismatic dislocation loops in zirconium and titanium.

As a result of the anisotropic distribution of dislocation lines and Burgers vectors in hcps, deviatoric straining of the crystal occurs as the dislocations climb and the loops grow. The segregation of vacancies and interstitials among grain boundaries of different orientations and between grain boundaries and dislocations also produce similar effects. Based on this, the irradiation-induced deformation of hcps associated with the corresponding evolution of the microstructure can be understood. Quantitative studies of irradiation growth in single-phase Zircaloy-2 have shown that the kinetic theory based on DAD can explain very well its dimensional behaviour under irradiation [84]. Accordingly, observations such as association of large growth rates in Zr and its alloys with the presence of *c*-component dislocations [85], and the 'anomalous' growth behaviour of flat grain Zr–2.5Nb material [49] can be understood readily.

7. Summary and conclusions

One of the important factors that differentiate the damage accumulation behaviour of different metals and alloys under different irradiation conditions is the crystal lattice structure. In this paper we describe the production and accumulation of irradiation damage, and its consequences on the physical and mechanical properties, of metals and alloys that crystallize in the hcp structure, in contrast to those in the cubic structure. The recent understanding of their complicated behaviour is also described.

In this regard, the usual rate theory model for cubic metals, which assume the isotropic diffusion of point defects, do not accurately reflect the reaction kinetics of point defects in the hcp metals. The diffusion anisotropy difference (DAD) between vacancies and interstitials can produce a bias among sinks that dominates the conventional dislocation bias. This effect adds a new dimension of complexity to the defect accumulation behaviour in hcp metals, and is found to be a major factor that causes the large difference in the damage accumulation behaviour between the hcps and the cubic metals.

Acknowledgements

The author is grateful for the funding support from the Research Grant Council of Hong Kong.

References

[1] D. Bacon, J. Nucl. Mater. 159 (1988) 176.
[2] W. Frank, Philos. Mag. A 63 (1991) 897.
[3] W. Frank, J. Nucl. Mater. 159 (1988) 122.
[4] A. Seeger, Philos. Mag. A 64 (1991) 735.
[5] G.M. Hood, H. Zhou, D. Gupta, R.J. Shultz, J. Nucl. Mater. 233 (1995) 122.
[6] R.A. Johnson, J.R. Beeler, in: J.K. Lee (Ed.), Interatomic Potentials and Crystalline Defects, AIME, New York, 1981, p. 165.
[7] W. Schilling, J. Nucl. Mater. 69/70 (1978) 465.
[8] H. Ullmaier, W. Schilling, in: Physics of Modern Materials, International Atomic Energy Agency, Vienna, 1980, p. 301.
[9] N.Q. Lam, N.V. Doan, L. Dagens, J. Phys. F 15 (1985) 799.
[10] C.H. Woo, B.N. Singh, Phys. Stat. Sol. B 159 (1990) 609.
[11] C.H. Woo, B.N. Singh, J. Nucl. Mater. 179–181 (1991) 1207.
[12] C.H. Woo, B.N. Singh, Philos. Mag. A 65 (1992) 889.
[13] S.J. Wooding, D.J. Bacon, Philos. Mag. A 76 (1997) 1033.
[14] A.G. Mikhin, N. De Diego, D.J. Bacon, Philos. Mag. A 75 (1997) 1153.
[15] D. Bacon, J. Nucl. Mater. 251 (1988) 176.
[16] C.H. Woo, B.N. Singh, H. Heinisch, J. Nucl. Mater. 174 (1990) 190.
[17] C.H. Woo, J. Nucl. Mater. 159 (1988) 237.
[18] C.H. Woo, Philos. Mag. 63 (1991) 915.
[19] H. Foll, M. Wilkens, Phys. Stat. Sol (a) 31 (1975) 519.
[20] V. Levy, J. Microsc. 19 (1974) 1.
[21] A. Jostons, R.G. Blake, J.G. Napier, P.M. Kelly, K. Farrell, J. Nucl. Mater. 68 (1977) 267.
[22] M. Griffiths, D. Faulkner, R.C. Styles, J. Nucl. Mater. 119 (1983) 189.
[23] W.J. Phythian, C.A. English, D.H. Yellen, D.J. Bacon, Philos. Mag. A 63 (1991) 821.
[24] M. Griffiths, M.H. Loretto, R.E. Smallman, Philos. Mag. A 49 (1984) 613.
[25] M. Griffiths, J. Nucl. Mater. 159 (1988) 190.
[26] M.E. Whitehead, A.S.A. Karim, M.H. Loretto, R.E. Smallman, Acta. Metall. 26 (1978) 983.
[27] A. Jostsons, P.M. Kelly, R.G. Blake, K. Farrell, ASTM STP 683 (1979) 46.
[28] A. Jostons, P.M. Kelly, R.G. Blake, J. Nucl. Mater. 66 (1977) 236.
[29] M. Griffiths, R.W. Gilbert, C.E. Coleman, J. Nucl. Mater. 159 (1988) 405.
[30] A. Jostsons, K. Farrell, Radiat. Eff. 15 (1972) 217.
[31] D. Faulkner, C.H. Woo, J. Nucl. Mater. 90 (1980) 307.
[32] M. Griffiths, D. Faulkner, R.C. Styles, J. Nucl. Mater. 119 (1983) 189.
[33] J.L. Brimhall, G.L. Kulchinski, H.E. Kissinger, B. Mastel, Radiat. Eff. 9 (1971) 273.
[34] M. Griffiths, Philos. Mag. A 63 (1991) 835.

[35] C.H. Woo, R.A. Holt, M. Griffith, in: Materials modeling: From Theory to Technology, Institute of Physics, Bristol, 1992, p. 55.
[36] P.T. Nettley, H. Bridge, J.H.S. Simmons, J. Brit. Nucl. Energy Soc. 2 (1963) 276.
[37] B.T. Kelly, in: Second Conference On Industry Carbon and Graphite, Society of Chemical Industry, London, 1966.
[38] P.T. Nettley, J.E. Brocklehurst, W.H. Martin, J.H.S. Simmons, Advanced and High-temperature Gas Cooled Reactors, IAEA, Vienna, 1969, p. 603.
[39] B.T. Kelly, B.S. Gray, W.H. Martin, V.C. Howard, M.J. Jenkins, Society of Chemical Industry, London, 1966, p. 499.
[40] Proceedings of the International Conference on Peaceful Uses of Atomic Energy, vol. 7, Geneva, 1955, United Nations, 1956.
[41] S.N. Buckley, Properties of Reactor Materials and Effects of Irradiation Damage, Butterworths, London, 1962, p. 413.
[42] G.J.C. Carpenter, C.E. Coleman, S.R. MacEwen (Eds.), Fundamental Mechanisms of Radiation Induced Creep and Growth, J. Nucl. Mater. 90 (1980).
[43] ASTM STP 633 (1977).
[44] C.H. Woo, R.J. McElroy (Eds.), Fundamental Mechanisms of Radiation Induced Creep and Growth, J. Nucl. Mater. 159 (1988).
[45] C.H. Woo, J. Nucl. Mater. 131 (1985) 105.
[46] C.H. Woo, in: Proceedings of the International Conference on Materials for Nuclear Reactor Core Applications, BNES, London, 1987, p. 65.
[47] V. Fidleris, J. Nucl. Mater. 159 (1988) 22.
[48] B.A. Cheadle, R.A. Holt, V. Fidleris, A.R. Causey, V. Urbanic, ASTM STP 754 (1982) 193.
[49] R.G. Fleck, R.A. Holt, V. Perovic, J. Tadros, J. Nucl. Mater. 159 (1988) 75.
[50] A. Rogerson, J. Nucl. Mater. 159 (1988) 43.
[51] A. Jostsons, P.M. Kelly, R.G. Blake, K. Farrell, ASTM STP 683 (1979) 46.
[52] R.A. Holt, R.W. Gilbert, J. Nucl. Mater. 137 (1986) 185.
[53] R.A. Holt, J. Nucl. Mater. 159 (1988) 310.
[54] R.P. Tucker, V. Fidleris, R.B. Adamson, ASTM STP 804 (1984) 427.
[55] W.M. Sloss, A. Davidson, TRG-Memo Report-6308, 1973.
[56] E. Edmonds, W. Sloss, K.Q. Bagley, W. Batey, in: Proceedings of the International Conference on Fast Breeder Reactor Fuel Performance Monterey, 1979, pp. 54–63.
[57] C. Brown, R.M. Sharpe, E.J. Fulton, C. Cawthorne, in: Proceedings of the Symposium on Dimensional Stability and Mechanical Behaviour of Irradiated metals and alloys, British Nuclear Energy Society, London, 1983, pp. 63–67.
[58] D.L. Porter, E.L. Wood, F.A. Garner, ASTM STP 1046 (2) (1990) 551.
[59] M. Griffiths, J. Nucl. Mater. 205 (1993) 225.
[60] R.B. Adamson, ASTM STP 633 (1977) 326.
[61] M. Griffiths, R.A. Holt, A. Rogerson, J. Nucl. Mater. 225 (1995) 245.
[62] G.M. Hood, R.J. Shultz, Mater. Sci. Forum 745 (1987) 15–18.
[63] M. Eldrup, G.M. Hood, N.J. Pedersen, R.J. Shultz, Mater. Sci. Forum 997 (1992) 105.
[64] C.K. Chow, C.H. Woo, unpublished data.
[65] R.A. Holt, J. Nucl. Mater. 159 (1988) 310.
[66] C.N. Tome, N. Christodoulou, P.A. Turner, M.A. Miller, C.H. Woo, J. Root, T.M. Holden, J. Nucl. Mater. 227 (1996) 237.
[67] C.H. Woo, U. Goesele, J. Nucl. Mater. 119 (1983) 219.
[68] C.H. Woo, ASTM STP 955 (1987) 70.
[69] R.A. Holt, C.H. Woo, C.K. Chow, J. Nucl. Mater. 205 (1993) 293.
[70] M.V. Smoluchowsk, Z. Phys. Chem. 92 (1917) 219.
[71] L. Onsager, Phys. Rev. 54 (1938) 554.
[72] P. Debye, Trans. Electrochem. Soc. 82 (1942) 265.
[73] T.R. Waite, Phys. Rev. 107 (1957) 463.
[74] U. Goesele, A. Seeger, Philos. Mag. 34 (1976) 177.
[75] H.S. Carlslaw, J.C. Jaeger, Conduction of Heat in Solids, Oxford University, Oxford, 1959.
[76] U. Goesele, Prog. Reaction Kinetics 13 (1984) 63.
[77] U. Goesele, J. Nucl. Mater. 78 (1978) 83.
[78] D.O. Northwood, R.W. Gfibert, L.E. Bahan, P.M. Kelly, R.O. Blake, A. Jostons, P. Madden, D. Faulkner, W. Bell, R.B. Adamson, J. Nucl. Mater. 79 (1979) 379.
[79] A. Jostsons, R.G. Blake, P.M. Kelly, Philos. Mag. A 41 (1980) 903.
[80] M. Chiffith, C.D. Cann, R.C. Styles, J. Nucl. Mater. 149 (1987) 200.
[81] C.H. Woo, W. Frank, J. Nucl. Mater. 137 (1985) 7.
[82] C.H. Woo, W. Frank, J. Nucl. Mater. 140 (1986) 214.
[83] C.H. Woo, W. Frank, J. Nucl. Mater. 148 (1987) 121.
[84] C.H. Woo, Rad. Effects and Defects in Solids 144 (1998) 145.
[85] R.A. Holt, R.W. Gilbert, J. Nucl. Mater. 137 (1986) 185.
[86] M. Griffiths, R.C. Styles, C.H. Woo, F. Phillipp, W. Frank, J. Nucl. Mater. 208 (1994) 324.